Optical properties of cubic boron nitride

M. I. Eremets,* M. Gauthier, A. Polian, J. C. Chervin, and J. M. Besson
Physique des Milieux Condensés, CNRS (URA 782), Université Pierre et Marie Curie, Boîte Postale 77, 4 place Jussieu, F-75252 Paris CEDEX 05, France

G. A. Dubitskii and Ye. Ye. Semenova
High Pressure Physics Institute, Academy of Sciences of Russia, 142092, Troitsk, Russia
(Received 13 February 1995)

Optical properties of cubic boron nitride were studied in the spectral range from 400 to 50 000 cm^{-1}. Raman-scattering, absorption, and reflection spectra were measured. The regions of the one-phonon and multiphonon absorption were studied in detail and the energies of the phonons were determined. The dispersion of the refractive index in the range 400–28 000 cm^{-1} was obtained from measurements of interference spectra on plateletlike samples. A model including one-phonon and Sellmeier electron oscillators was used to fit the dispersion of the refractive index. Both the static and high-frequency dielectric constants ε_0 and ε_∞ were obtained and found to be 6.80 and 4.46, respectively. The parameters of the phonon oscillators were used for simulation of the interference spectra in transmission and reflection. Techniques for preparing free-standing samples of dimensions of the order of 150×150 μm and of thickness down to 0.2 μm are described as well as methods to measure their thickness.

I. INTRODUCTION

Cubic zinc-blende boron nitride (*c*-BN) is synthesized at pressures above 4.5 GPa and temperatures above 1500 K. It is a very important material because of its hardness, which is second only to diamond, its high thermal conductivity, high melting temperature, large band gap, low dielectric constant, and low reactivity. When the problems of crystal growth are solved (to our knowledge, the largest samples of *c*-BN are less than 1 mm across), it will be a good material for electronics.[1,2]

c-BN is the lightest of the III-V semiconductors. It is a relatively simple substance, and numerous calculations of its lattice and electronic properties exist.[3] By contrast, probably due to the difficulty in growing large single crystals, comparatively few experimental results are available on its optical properties. Miyata *et al.*[4] determined the optical constants in the spectral region 2–23 eV (16 000–185 000 cm^{-1}) from reflection and transmittance measurements. The fundamental indirect band gap determined in this study is $E_g=6.4\pm0.5$ eV. *c*-BN has almost no absorption from the fundamental gap down to the infrared region, where a strong reststrahlen band is observed. Information on the strength of the chemical bond and on the refractive index exists.[5,6] The difference between the frequencies of the TO and LO modes indicates a sizable ionicity. But the values of the LO (1340 cm^{-1}) and TO (1056 cm^{-1}) modes deduced from the infrared reflectivity spectra by a fit in a one-oscillator approximation[6] differ from the Raman determination: 1306 and 1056 cm^{-1}, respectively.[7,8] The dispersion of the refractive index was deduced from a Kramers-Kronig analysis of a reflectivity spectrum of a compacted polycrystalline sample[6] ($\varepsilon_\infty=4.5$ and $\varepsilon_0=7.1$). The refractive index has been obtained in limited spectral regions in the visible region of the spectrum by matching the indices of BN and melts of sulfur and selenium at 10% weight intervals.[6] Theoretical works give $\varepsilon_\infty=4.94$ (Ref. 9) or $\varepsilon_\infty=3.86$.[3]

Weaker absorption bands around 2000 cm^{-1} were assigned to two-phonon absorption, but there is a large discrepancy between the assignment of the peaks by Gielisse *et al.*[6] and by Chrenko.[5] The dispersion of the phonons was investigated neither theoretically nor experimentally. Only very recently were elastic constants at ambient conditions measured.[10]

From the above, it is clear that the optical properties of *c*-BN are poorly determined, and this provides further motivation to reexamine these properties in the visible and infrared regions.

II. EXPERIMENT

The single crystals of cubic boron nitride used in this study were prepared from the system BN_{hex}-LiH.[11] Most of the experiments were done with transparent, colorless, or slightly brown single crystals. The samples were approximately hexagonal platelets with a thickness between 1 and 20 μm and a diameter from 10 to 200 μm. High-quality yellow transparent crystals, with slightly larger dimensions (thickness 15–50 μm and overall dimensions 100–200 μm) were also used.

Very thin plateletlike samples of thicknesses down to 0.2 μm (starting thickness 1–5 μm) were prepared by argon-ion milling with an etching rate of approximately 0.5 μm/h. An angle of 15° between the ion beam and the plane of the sample was chosen to provide a smooth etching. The surface of the etched samples remains flat even after removing $\approx$5-μm-thick layer. Free-standing high-quality 150×150-μm samples with 0.45-μm thickness were prepared in such a way.

0163-1829/95/52(12)/8854(10)/$06.00

Reflectivity and transmission measurements were made in the region of 400–4000 cm^{-1} [Figs. 1(a) and 1(b)], with a Perkin-Elmer 1600 (PE) Fourier transform infrared (FTIR) spectrometer equipped with an infrared microscope, consisting of two Cassegrain mirror objectives (24-mm working distance, ×6, 0.60 numerical aperture, and a 38° optical aperture with 18° blind cone). Interference transmittance spectra between 400 and 20 000 cm^{-1} were obtained with a BOMEM (*B*) FTIR spectrometer and with a Jobin-Yvon (JY) grating spectrometer from 8000 to 50 000 cm^{-1}.

For transmission measurements, the samples were placed on a hole 15–20 μm in diameter made in a $\approx$10-μm-thick Al foil. Suitable signals were obtained even through a 10-μm-diameter hole with the PE instrument. Reference spectra were recorded through the same hole without any sample. For the reflectivity measurements the samples were placed on a BaF_2 substrate. The reflection of an Al mirror was used for the 100% reference.

Larger samples were placed on a hole of diameter $\approx$100 μm without any substrate, and transmission and reflection spectra were measured at the same place of the sample. The area of the sample used for measurements was selected with a measuring field diaphragm. Thus absolute values of transmission and reflection were obtained.

Measuring the thickness of a sample with dimensions $\leq$100 μm is a problem in itself. In order to determine as precisely as possible the thickness of the samples, three independent procedures were used.

In the first procedure, a scanning electron microscope (JEOL JSM-840AIt) was used. The very large depth of focus ($1 \approx 50$ mm) enables us to rotate the sample together with the microscope support by 90° with respect to the electron beam and to observe or photograph the image of the sample profile in scale. The sample was placed without any glue on a polished sapphire surface, and the sample together with the sapphire support was covered with a semitransparent gold film. This arrangement was also used for interference measurement of thickness in the visible range (see below). With this technique, the thickness of a sample could be measured with a precision of $\sim 1\%$. By rotating the sample, it was possible to measure the thickness of the various edges. In the present experiment, all results were the same within the precision of the measurement, showing that the opposite faces were parallel.

Another method is to determine the thickness from the interference spectrum which is obtained when light is focused onto an edge of the sample. Interferences do appear between the light reflected from the sample surface and that reflected from the substrate surface. The usual formula for interferences is $2nev=m$, where e is the height of the step, ν the frequency of the interference maximum of order m, and $n=1$. This method will be described in detail elsewhere. In the present case, the interference is formed in air without dispersion and a simple formula $2e(\nu_1-\nu_2)=\Delta m$, where Δm is the number of extrema between ν_1 and ν_2, is used to obtain the thickness. In this way, the thickness of a sample was mea-

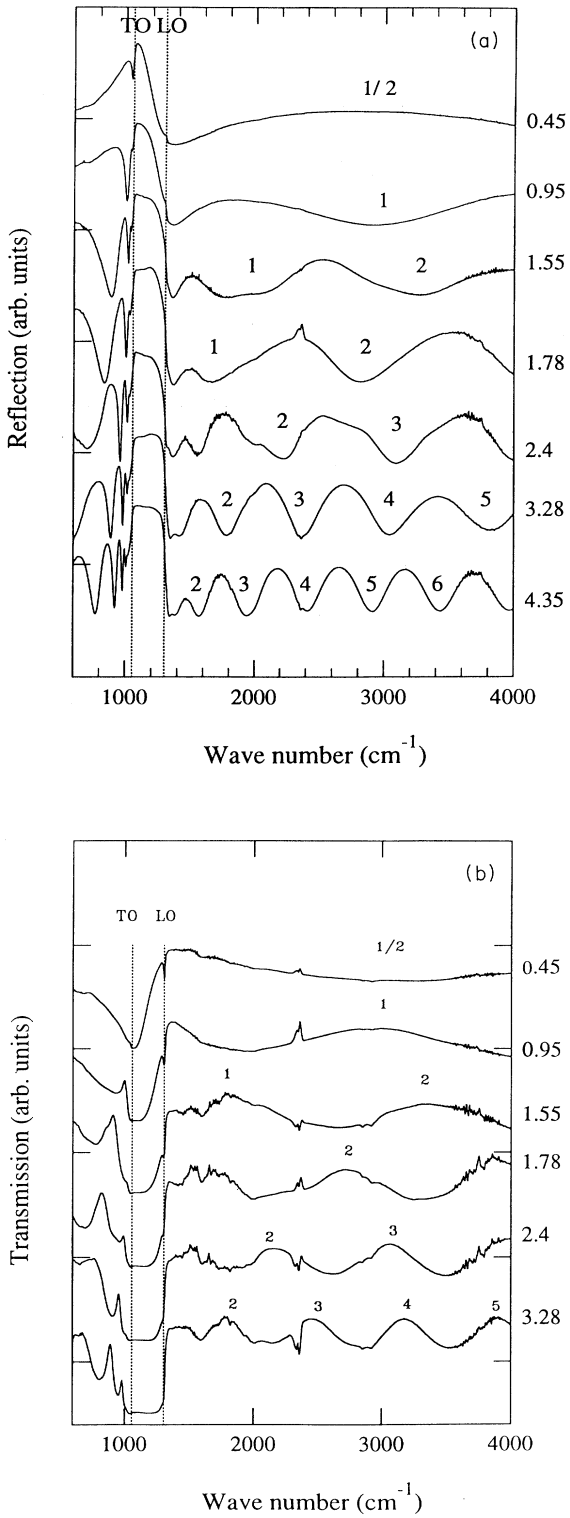

FIG. 1. Reflection (a) and transmission (b) spectra of samples of various thicknesses. The numbers on the interference minima (reflection) or maxima (transmission) are the interference orders. The thickness of the sample in μm is shown on the right-hand side of the figure. The peaks around 2400 cm^{-1} originate from the absorption of the atmospheric CO_2. Spectra are shifted vertically relative to each other for clarity.

sured ($d=37.6$ μm) with an accuracy better than 1% at various points on different sides of the sample.

The third technique consists of measuring the angular dependence of the interference spectrum, and will be described in the paragraph concerning the absolute calibration of the refractive index.

III. RESULTS AND DISCUSSION

The fundamental gap of c-BN is equal to $E_g=6.4\pm0.5$ eV.[4,5] The present measurements were performed only up to 6 eV, and hence the absorption edge was not observed. At energies below the fundamental gap, c-BN shows strong absorption only in the reststrahlen region, and around 2000 cm^{-1} which is assigned to multiphonon absorption. In this work we studied in detail the one-phonon absorption region and determined the refractive index in the whole spectral range. Information about phonons in c-BN was obtained from Raman measurements, reststrahlen absorption, and two-phonon absorption.

c-BN crystallizes in the zinc-blende structure with two atoms in the unit cell. Thus the phonons are both Raman and IR active. The sharp Raman peaks in our samples at 1304.8 and 1055.7 cm^{-1} correspond to LO(Γ) and TO (Γ) respectively, and are consistent with the published values.[7,8] In some samples additional peaks at 1276.1 and 1260.9 cm^{-1} were observed, which must be related to local impurity modes.

Because of the transverse nature of light, there is no absorption by LO modes at normal incidence. We very clearly observed LO modes in the transmission spectra of samples of thickness less than 2 μm [Fig. 1(b)], because the beam is not perpendicular to the surface due to the Cassegrain objective as explained by Berreman.[12]

The LO-mode absorption becomes stronger when the sample rests on a metallic substrate, because of the phase change of the light reflected from a metallic surface. In particular, the 1.1-μ-thick sample shows very sharp peaks. These peaks could eventually be used as a gauge for pressure or temperature measurements in the infrared region where there is no versatile gauge.

The TO mode was observed in transmission spectra only in films of ionic crystals sputtered on a substrate,[12] or epitaxially grown layers[11,13] of semiconductors. We observed it both in reflection and transmission in the free-standing sample of thickness ≈0.45 μm [Figs. 1(a) and 1(b)].

The absorption is rather strong in the reststrahlen range, $\alpha=10^4-10^5$ cm^{-1}, and the optical constants, the extinction coefficient κ, and the refractive index n are usually obtained from the reflectivity spectra through a Kramers-Kronig (KK) analysis. The spectra were smoothed out but in the region of the reflectivity peak (1000–1300 cm^{-1}) to keep the sharp structure of n and κ after the KK transformation. Perfect smoothing does not exist, and therefore the spectra of n and κ have some features. Nevertheless, KK analysis shows the general characteristics of the optical properties of c-BN which are determined by a one-phonon oscillator with $\omega_{TO}\approx1050$ cm^{-1} and $\omega_{LO}\approx1310$ cm^{-1}. This treatment requires reflectivity measurements in a large frequency range. The sample has to be flat and thick, and the incident beam has to be normal to the surface of the sample. Moreover, limiting values of the high- and low-frequency reflectivities have to be known. Due to the size of the available samples, it is difficult to fulfill all these requirements with c-BN and therefore to determine the optical constants precisely by this method. Hence we used interference measurements, both in reflection and in transmission, and fitted the data with a model including the phonon and a Sellmeier one-electron oscillator.

The measured two-phonon absorption spectrum is similar to that obtained by Chrenko,[5] and to the less well-resolved spectrum obtained by Gielisse.[5] A sharp and intense peak at 1818 cm^{-1} is intrinsic to c-BN but is not yet identified. This peak is probably not a local mode because it has the same frequency in samples of different origins.

Interference spectra

The interaction of light with a medium is expressed through the complex refractive index $n-i\kappa$. To determine n and κ, the transmission (T) and reflection (R) spectra were measured. Different couples of experimental data such as T_1 and T_2 (samples of different thicknesses) or T and φ (phase of light) will also yield n and κ.[14] The usual formulas for reflectivity and transmittance from which n and κ can be calculated are complicated. We used the simpler general equations proposed by Heavens[14] for the case where the incident light is normal to a film of thickness d and complex refractive index $n_1-i\kappa_1$, located in a nonabsorbing medium of refractive index n_0 and resting on a substrate of complex refractive index $n_2-i\kappa_2$. In this case, the reflection and transmission are given by

$$R=\frac{(g_1^2+h_1^2)\exp(2\alpha_1)+(g_2^2+h_2^2)\exp(-2\alpha_1)+A\cos2\gamma_1+B\sin2\gamma_1}{\exp(2\alpha_1)+(g_1^2+h_1^2)(g_2+h_2^2)\exp(-2\alpha_1)+C\cos2\gamma_1+D\sin2\gamma_1}, \tag{1}$$

$$T=\frac{n_2}{n_0}\frac{\{(1+g_1)^2+h_1^2\}\{(1+g_2)^2+h_2^2\}}{\exp(2\alpha_1)+(g_1^2+h_1^2)(g_2^2+h_2^2)\exp(-2\alpha_1)+C\cos2\gamma_1+D\sin2\gamma_1}, \tag{2}$$

where

$$A=2(g_1g_2+h_1h_2),\quad B=2(g_1h_2-g_2h_1),$$
$$C=2(g_1g_2-h_1h_2),\quad D=2(g_1h_2+g_2h_1),$$
$$g_1=\frac{n_0^2-n_1^2-\kappa_1^2}{(n_0+n_1)^2+\kappa_1^2},\quad h_1=\frac{2n_0\kappa_1}{(n_0+n_1)^2+\kappa_1^2},$$
$$g_2=\frac{n_1^2-n_2^2+\kappa_1^2-\kappa_2^2}{(n_1+n_2)^2+(\kappa_1+\kappa_2)^2},\quad (3)$$
$$h_2=\frac{2(n_1\kappa_2-n_2\kappa_1)}{(n_1+n_2)^2+(\kappa_1+\kappa_2)^2},$$
$$\alpha_1=2\pi\kappa_1 d\nu,\quad \gamma_1=2\pi n_1 d\nu.$$

These equations describe the transmission and reflection spectra of samples deposited on various substrates.

If the thickness d of the sample is determined, and its reflection R and transmission T measured under normal incidence, it is possible to derive n and κ from these equations. In practice, it is difficult because the system of equations (1) and (2) has multiple solutions and because the absolute values of R and T must be known accurately. Fortunately, it is often possible to determine n and κ separately in the spectral regions of transparency and absorption, where these formulas are drastically simplified. Equations (1)–(3) in the complete form are very useful, because they successfully describe the case of samples having a complicated dispersion in the geometry of the platelet samples resting on different substrates including metallic ones. This simulation helps, in particular, to determine precisely the thickness of a sample from a fit with the interference spectrum.

The Fabry-Perot interference fringe method is one of the few methods available to measure the refractive index of thin samples. In this case the sample is prepared in platelet form and the interference pattern is observed in transmission or reflection. With this method it is quite easy to obtain an interference pattern. It is also very easy to make systematic errors. Therefore a large part of the present work was devoted to obtaining reliable and unambiguous data. Special attention was paid to the overlap of the dispersion curves obtained for different samples in different spectral ranges.

In the case of low absorption, Eqs. (1)–(3) are very simple: when the sample is surrounded by a medium of smaller refractive index, reflection minima (or maxima in transmission) correspond to

$$2n_1(\nu)d\nu=m\,(m\text{ integer}).\quad (4)$$

This equation is widely used to obtain the dispersion of the refractive index. The exact determination of the interference order m is the main difficulty of this technique. The most reliable method for determining it is to start with a very thin sample or a very long wavelength to identify unambiguously the interference order from the fringes (Fig. 1) and to determine the value of $n(\nu)d$ at the extrema. Note that equal values of m may be found on the right- and left-hand sides of a resonance where a jump occurs in the refractive index. Thus, using Eq. (4),

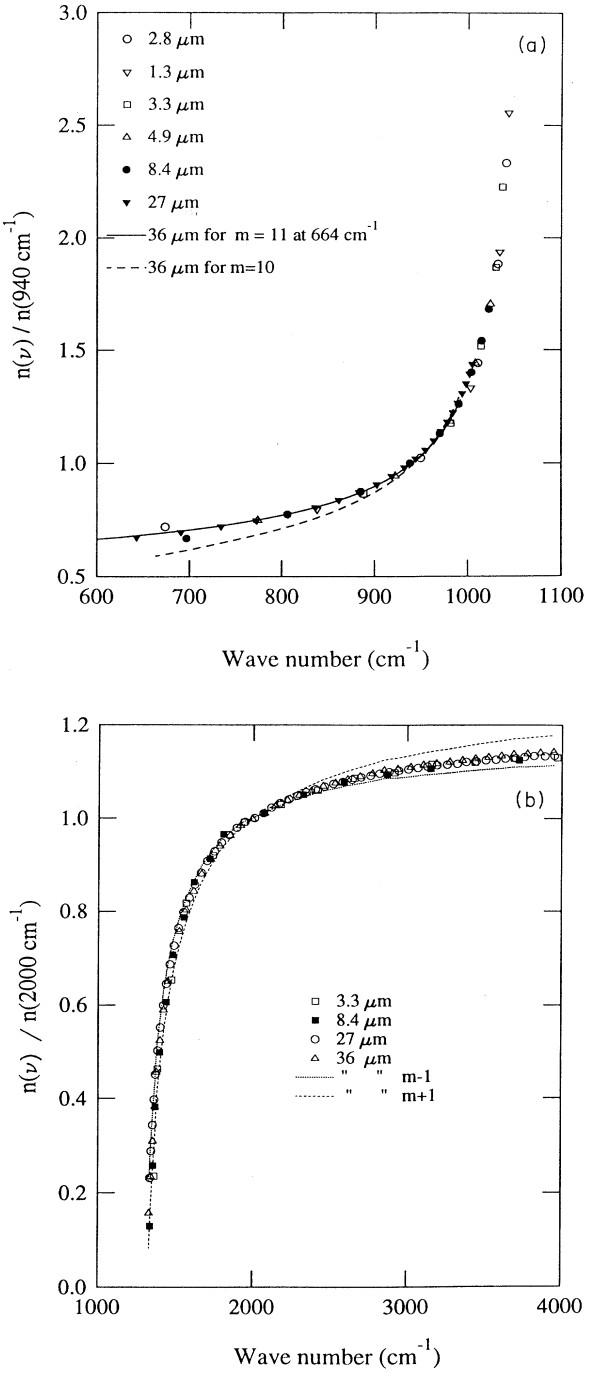

FIG. 2. (a) Dispersion of the low-frequency refractive index in relative units. Experimental points were calculated from the positions of the extrema and the interference orders shown through Eq. (4). To compare data from different samples of small ($\sim$1–5 μm) but unknown thicknesses, the inteference order at 940 cm^{-1} was tentatively assigned to $m=1$. On the basis of this dispersion curve the interference orders for thicker samples ($\sim$27- and $\sim$36-μm-thick samples) were determined, and the dispersion curves were also plotted. The dispersion curve determined with the interference order changed by 1 is shown by the dashed line. (b) Same as (a) at the right-hand high-frequency side of the resonance. The spectra were fitted with $m=1$ at $\nu=2000$ cm^{-1}.

$n(\nu)d$ for each sample can be deduced. We first arbitrarily assigned a value of $n=1$ at $\nu=940$ cm^{-1} and $n=1$ at 2000 cm^{-1}, and the dispersion of the relative index $n(\nu)d/n(\nu_0)d$ was obtained for each sample (Fig. 2). On the basis of this dependence, the assignment of the interference peaks for thicker samples was found from the known ratio of refractive index of peaks at ν_1 and ν_2 separated by counted difference or orders Δm. Thus a rather exact relative dispersion curve can be obtained for thick samples. The validity of the assignment can be checked by varying the obtained value of m and calculating the dispersion curve with Eq. (4) (Fig. 2) on the left- and right-hand sides of the resonance. The index-of-refraction curves were connected by scaling them with the help of the measured values of $n(940\ \text{cm}^{-1})d$ and $n(2000\ \text{cm}^{-1})d$ for the same sample.

When the thickness of a thick sample is determined (the thickness of very thin samples is more difficult to ascertain) the dispersion curve in absolute value is obtained. In general, the dispersion of the index in relative value can be obtained with greater accuracy than the absolute value of the thickness.

Note here that, because its values are discrete, this fitting procedure is rather sensitive to variations in m (Fig. 2) even for thick samples with large m. Therefore the following procedure of assignment of the order of interference m to one peak can be proposed. If two samples have different thicknesses, arbitrary starting values m_1 and m_2 are assigned to some of the peaks of the first and second samples, respectively. Then the dispersion curves are calculated, matched at some wavelength, and compared over the rest of the spectrum. Varying m_1 and m_2, the best fit is found which corresponds to the correct values of m_1 and m_2.

The above considerations are valid for measurements with a parallel beam. But for small samples a large magnification is needed and a convergent beam must be used. The positions of the extrema in the interference spectrum depend on the optical aperture of the objective lens. When the incident beam is at an angle θ with the surface, the interference condition becomes

$$2d\nu\sqrt{n(\nu)^2-\sin^2\theta}=m\ . \tag{5}$$

In other words, the measured value of the index (the average over the angles of aperture) is smaller than the actual one. The correction depends on the aperture of the objective and on the refractive index of the sample. It is especially important in the frequency range where the refractive index is small and when a large aperture objective is used (Fig. 3). For example, a correction of 3% has

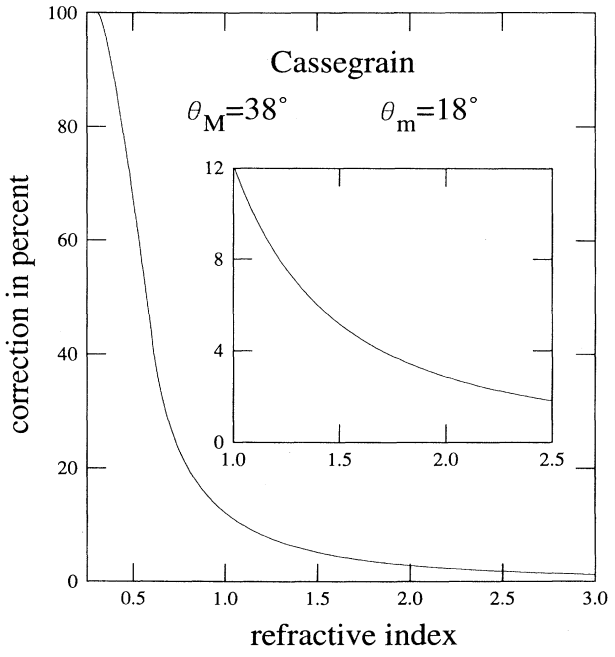

FIG. 3. Correction which has to be introduced in the dispersion curves (Fig. 2) because of the convergence of the beam of the PE spectrometer. The correction (increase of the refractive index) deduced from Eq. (5) depends on the refractive index. The correction is maximum in the region of the phonon resonance near the LO mode. θ_M is the optical aperture, and θ_m the blind cone of the Cassegrain objectives. The inset shows details of the correction for $1\le n\le 2.5$.

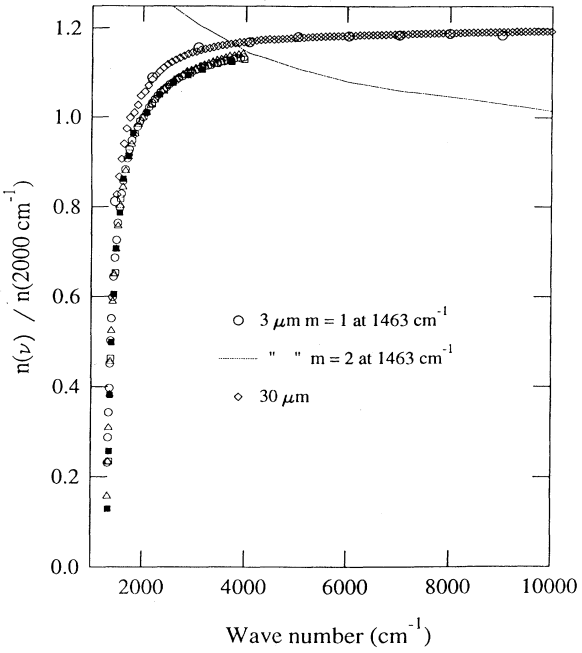

FIG. 4. Connection of the data obtained with the infrared 400–4000-cm^{-1} PE spectrometer with the data obtained with the B spectrometer (400–20 000 cm^{-1}). A correction of 3% was introduced for the infrared data at 4000 cm^{-1} according to Fig. 3. The dotted line shows the large deviation from the correct dependence when the order of interference is changd by one unit. The dispersion curve for the thick sample, $d\approx 30$ μm, was plotted on the basis of the dispersion obtained for the thin sample.

to be made around 4000 cm^{-1} where n is ≈ 2.

The refractive index data were corrected to connect IR dispersion curves with the data obtained with the B spectrometer in the range 400–20 000 cm^{-1} (Fig. 4). Transmittance spectra were recorded with this spectrometer with a rather small aperture of 4°, and therefore no angular correction was needed. The procedure for the determination of the refractive index dispersion in the IR and visible regions with the B spectrometer was the same as for the IR range. At first, the spectrum of a thin sample ($d \approx 3$ μm) was recorded for reliable assignment of the order of interference. Then the dependence of the refractive index (relative values) was determined. This fit was also checked by changing the interference order (Fig. 4). On the basis of this curve, the assignment of the interference spectrum for a thick sample ($d \approx 30$ μm) was done, and a more precise dispersion curve was obtained. Again, the validity of this fit was checked by varying the interference order m.

The next step in extending the dispersion curve to UV was the measurement of the spectra with the JY instrument. The contrast of the interference fringes was very good in the 10 000–20 000-cm^{-1} range, and decreased at higher frequency so that above 28 000 cm^{-1} the fringes disappeared. No angular correction was needed because of the small aperture (4°). The same fitting procedure was performed (Fig. 5) to determine the correct value of the interference order m.

Thus the dispersion curve in relative values over the whole range 400–28 000 cm^{-1} was accurately obtained. To determine this dependence in absolute values, it was sufficient to determine the thickness of one sample or to determine the value of the refractive index at one given frequency. We were able to measure the thickness of a sample with a precision of 1–2 % with the methods described in Sec. II, and both the thickness and refractive index by measuring the angular dependence of the interference spectrum: By tilting a sample one may vary the optical path length in the sample and thus its effective thickness. The main advantage of angular measurements is that they allow one to separate n and d, which always appear as a product in the equation for normal incidence. From Eq. (5), the absolute values of both n and d may be obtained exactly, if the order of interference is known. Equation (5) can be rewritten as

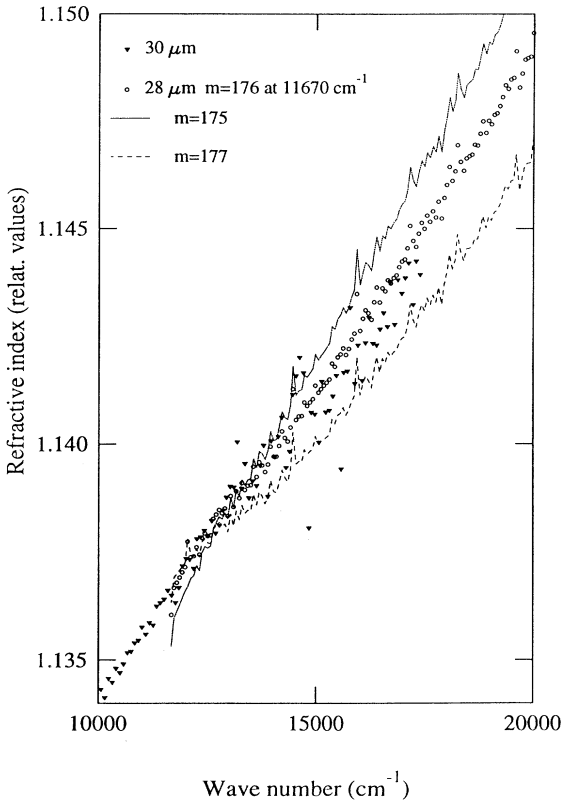

FIG. 5. Connection of the data obtained for a 30-μm-thick sample measured with the BOMEM instrument, with the data in visible region obtained for a 28-μm-thick sample with the Jobin-Yvon spectrometer. The best fit is achieved for the order of interference $m = 176$ at 11 670 cm^{-1}. The deviation from this fit when the order is changed by ± 1 is shown by dotted and dashed lines.

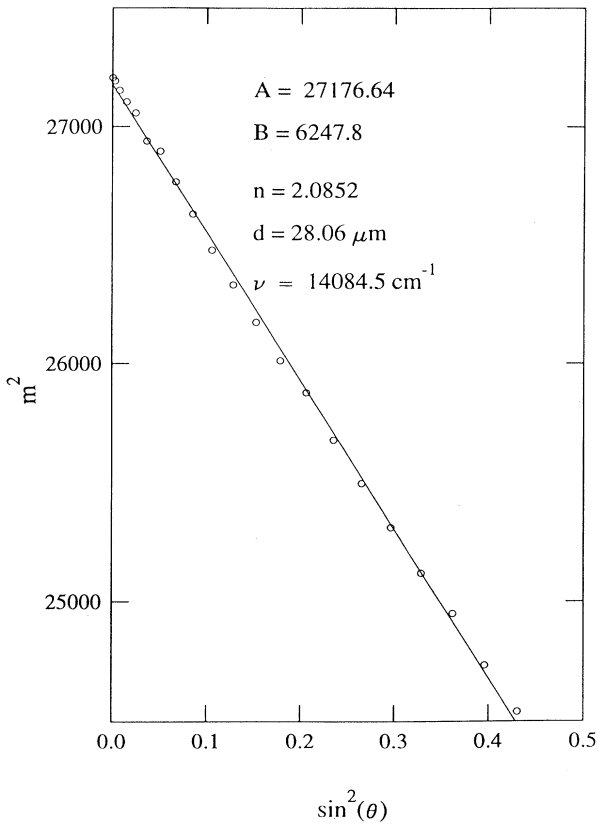

FIG. 6. Dependence of the interference order at 14 084.5 cm^{-1} with the angle between the normal to the sample and the direction of the light beam. From the slope of the line the thickness is determined, and from the vaue of m^2 at $\theta = 0$ the absolute value of the refractive index is evaluated [Eq. (6)].

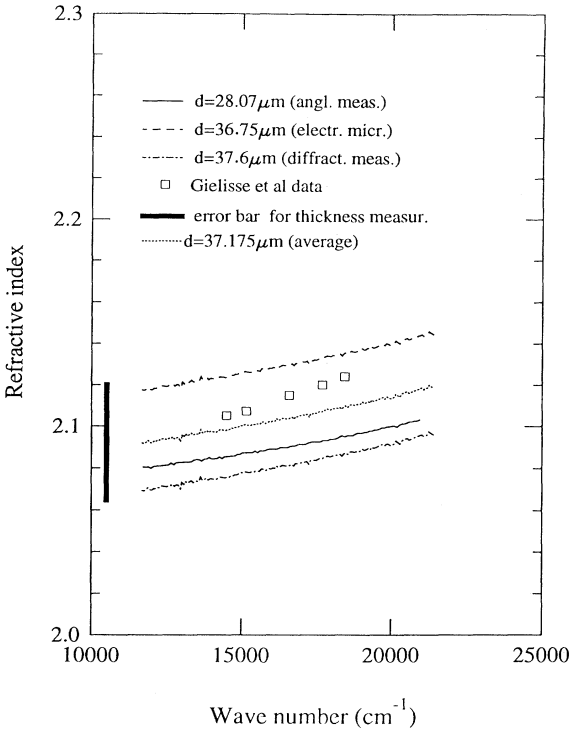

FIG. 7. Comparison of the absolute values of the refractive index obtained for two samples by different methods. Sample 1: thickness measurement with an electron microscope (dashed line), thickness measurements from interference (diffraction) on the edge ("step") of a sample (dash-dotted line), and averge value (dotted line). Sample 2: angular dependence measurements (continuous line). The results of Gielisse *et al.* (Ref. 6) are the empty squares. The maximum error on the refractive index coming from the thickness measurements is shown by the thick vertical line.

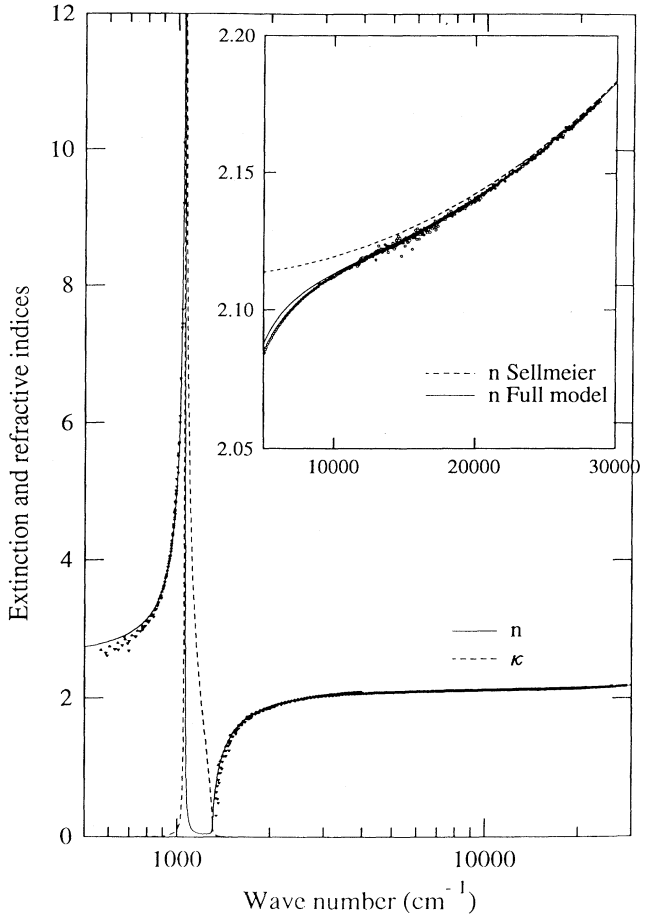

FIG. 8. Full data for the extinction coefficient (dashed line) and refractive index (continuous line) evaluated in the region 500–28 000 cm^{-1}. The inset represents a comparison of the experimental results with the full model (continuous line) and a Sellmeier oscillator only (dashed line).

$$m^2 = A - B\sin^2\theta, \quad A = 4d^2\nu^2 n^2, \quad B = 4d^2\nu^2 . \tag{6}$$

The slope of the linear dependence of m^2 as a function of $\sin^2\theta$ (Fig. 6) gives the thickness, and from A the refractive index is obtained. This approach is valid even when dispersion is present, because the measurements are made at a fixed wavelength. This method requires knowledge of the order of interference. To determine it, the relative dispersion curve for a given sample was fitted to the general dispersion curve in the same manner as shown in Fig. 5. The sample angle was measured on a goniometric head in the range $\pm 40°$.

The coincidence between these three methods of measurements is 2% (Fig. 7). It is difficult to estimate the systematic errors made by these methods of measurement. Therefore we simply averaged the values of the refractive indices obtained by these methods at 14 035 cm^{-1}, where the angular measurements were done. The average value of the refractive index at 14 035 cm^{-1} is $n = 2.097$. This value was used to scale the whole relative dependence of the refractive index, and the dispersion of the refractive index of cubic boron nitride was obtained in absolute values (Fig. 8) as explained in Sec. IV.

IV. DIELECTRIC FUNCTION OF *c*-BN

Interaction of light with a medium is described by the complex dielectric constant

$$\varepsilon = (n + i\kappa)^2 . \tag{7}$$

In the reststrahlen region, the real and imaginary parts are expressed as

$$\varepsilon' = n^2 - \kappa^2 = \varepsilon_\infty + \frac{(\varepsilon_0 - \varepsilon_\infty)(\omega_{TO}^2 - \omega^2)\omega_{TO}^2}{(\omega_{TO}^2 - \omega^2)^2 + \Gamma^2\omega^2} , \tag{8}$$

$$\varepsilon'' = 2n\kappa = \frac{(\varepsilon_0 - \varepsilon_\infty)\omega_{TO}^2\omega\Gamma}{(\omega_{TO}^2 - \omega^2)^2 + \Gamma^2\omega^2} , \tag{9}$$

where ε_0 is the static dielectric constant, ε_∞ the high-

frequency dielectric constant, ω_{TO} the transverse-optical mode at $k=0$, and Γ the damping constant. ε_0 and ε_∞ are connected through the Lyddane-Sachs-Teller relation

$$\varepsilon_\infty=\varepsilon_0\left[\frac{\omega_{TO}}{\omega_{LO}}\right]^2 . \tag{10}$$

The experimental determination of ε_0 is unambiguous: it is the limit for long wavelengths, but ε_∞ is not so well defined because in the high-frequency region there is an overlap with the dielectric contribution from electronic oscillators.

The dispersion of the real part of the dielectric constant reflects the existence of oscillators in the material. The refractive index at energies below the energy gap is built up from the contribution of the electronic transitions in the system. Usually the approximation is made of one or two predominant transitions. Wemple and DiDomenico[15] have shown that the dispersion of the refractive index of more than 100 ionic and covalent materials can be well described by a Sellmeier single oscillator

$$n(\omega)^2-1=\frac{F_1}{(\omega_1^2-\omega^2)} , \tag{11}$$

where F_1 is the oscillator strength and ω_1 is the oscillator frequency which correlates with the energy of direct valence-conduction-band transitions. Of course, the measured $n(\nu,P)$ cannot describe the detailed electronic structure, and theoretical first-principles calculations would have to be used. Also these measurements are not sensitive to indirect transitions which have smaller oscillator strengths.

We obtained the value of ε_0 by fitting the experimental curve with both contributions from the phonon oscillator and from the electronic transitions using a Sellmeier model. This equation can be written as

$$\varepsilon=\varepsilon_{ph}+\varepsilon_{elec}-\varepsilon_\infty , \tag{12}$$

with

$$\varepsilon_{elec}-1=\frac{\varepsilon_\infty-1}{1-\left[\hbar\omega/E_0\right]^2} \tag{13}$$

for the Sellmeier contribution (11) which verifies $\varepsilon_{elec}\to\varepsilon_\infty$ when $\omega\to 0$, and $\varepsilon_{elec}\to 1$ when $\omega\to\infty$. The whole set of experimental data was fitted with this model using only two free parameters: ε_0 and E_0. The damping parameter Γ could also vary, but it influences only the values of n and κ at the maxima; $\Gamma=0.005$ was found to give a satisfactory fit. The exact values of the TO- and LO-mode frequencies were taken from the Raman measurements. Thus $\varepsilon_0=6.80$ and $E_0=104\,850$ cm^{-1} (13 ± 0.05 eV) were obtained. The result is compared with experiment in Fig. 8. The fit is well within experimental uncertainty except below 700 cm^{-1}, where refractive index values are lower than the calculated values by almost 5%. This might be accounted for by using a smaller value for ε_0. Nevertheless, this is not possible since ε_0 and ε_∞ are very tightly related by the Lyddane-Sachs-Teller (LST) relation and the experimental values

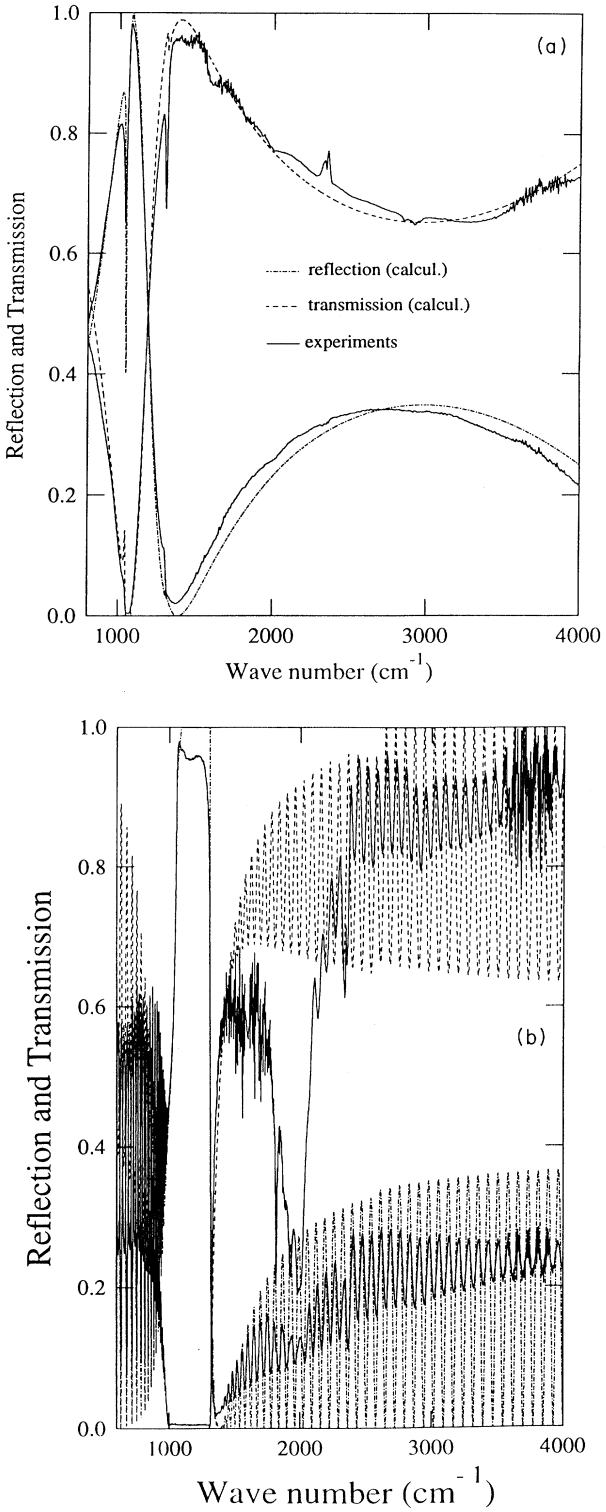

FIG. 9. (a) Comparison of the simulated reflection (dashed line) and transmission spectra (dashed-dotted line) using Eq. (1)–(3) with the experimental results (continuous lines). The parameters used in the simulation are $\varepsilon_0=6.80$, $E_0=13$ eV, $\omega_{TO}=1055.7$ cm^{-1}, $\omega_{LO}=1304.8$ cm^{-1}, and $\Gamma=0.005$. The thickness of the slab is 0.45 ± 0.02 μm. (b) Same as (a), using the same parameters for the simulation. The thickness is 31.03 ± 0.02 μm.

of ω_{LO} and ω_{TO}. If ε_0 is taken to be lower than 6.80 to accommodate the low-energy part of the refractive index spectrum, this throws off the fit over the rest of the entire spectrum, well outside the experimental uncertainty. We therefore propose this value of 6.8 to be the true value for pure BN. The discrepancy between the calculated curve and the experimental value for n may be accounted for by lower-lying oscillators, possibly due to shallow residual impurities and/or free carriers. This is not unexpected, in view of the large number of impurities and nonstoichiometric defects which are usually found in c-BN material. From the LST relationship it follows that $\varepsilon_\infty=4.46$. E_0 corresponds to the peak observed in the UV reflectivity spectrum.[4] As expected, the contribution of the gap is negligible. From the values of the longitudinal- and transverse-optical-phonon frequencies, and from the static and dynamic dielectric constants, it is easy to deduce the transverse effective e^* and the Szigeti effective charge e_s charge from the oscillator strength from [in the Système International (SI)]

$$(\varepsilon_0-\varepsilon_\infty)\omega_{TO}^2=\frac{Ne^{*2}}{M}\ , \tag{14}$$

and

$$e_S=\left[\frac{3}{\varepsilon_\infty+2}\right]e^*\ , \tag{15}$$

where $N=k/V$, $k=4$ is the number of dipoles in the unit cell of volume V, and M the reduced mass, i.e., $M=M_BM_N/(M_B+M_N)$. Using the values found in the present study, one obtains $e_S=0.91e$ and $e^*=1.96e$. These values show that BN is a very ionic compound,[16] with an effective charge of the same order of magnitude as ZnO, ZnS, or RbCl. Moreover, it is worth noting that the oscillator strength is extremely high in BN ($\sim 2\times 10^6$ cm^{-2}), which is approximately three times as much as that of a very ionic compound such as LiF.

From the dispersion of n and κ, it is possible to model the absorption and reflection spectra. We found that Eqs. (1)–(3) describe very well the experimental spectra of all the samples as shown in Fig. 9. In order to obtain the calculated curves in Figs. 9(a) and 9(b), only the thickness was varied. The fit is very sensitive to this value and therefore the thickness of a c-BN sample can be determined very accurately, much more precisely than from the positions of the interference peaks.

The spectra were also successfully simulated for samples on a metallic substrate. One of the samples was placed on the copper substrate and etched with argon-ion milling, down to a thickness of 0.2 μm. This value of the thickness was obtained from the fit of the spectrum. The fitting procedure is very useful for precise etching of the sample. The spectrum of the sample can be recorded without transferring it onto a transparent substrate. It seems that this method would allow one to prepare free-standing samples of thicknesses below 0.1 μm.

V. CONCLUSIONS

The optical properties of cubic boron nitride were studied from the far infrared to the near ultraviolet. The phonons in c-BN were evaluated from Raman scattering and from one-phonon and multiphonon absorption. The dispersion of the refractive index through the whole spectral region of transparency was obtained from interference spectra on slabs of c-BN. The dispersion curve was fitted with a model including the phonon and the electron Sellmeier oscillators. The parameters of the oscillators were obtained. In particular, the static dielectric constant was obtained and found to be equal to $\varepsilon_0=6.80$. The transmission and reflection spectra were precisely fitted using the determined parameters. The determination of the static and high-frequency dielectric constants enabled the calculation of the effective charges. It was shown that c-BN is a very ionic compound.

The very thin samples needed for this work were prepared by thinning the starting samples down by ion etching. High-quality monocrystalline free-standing samples with a large area $\approx 150\times 150$ μm^2 and a thickness down to 0.2 μm could be prepared. This thickness does not seem to be a lower limit, and thinner samples certainly could be prepared by this method. The absorption peak at the energy of the TO mode was clearly resolved in such samples.

ACKNOWLEDGMENTS

We would like to thank V. B. Shipilo, L. M. Gamezo, and A. I. Lukomskii for the samples of c-BN used in some experiments. We are indebted to R. LeToullec, P. Loubeyre, and J. P. Pinceaux for use of their setup and fruitful discussions, and C. Naud and C. Porte for the use of their setup. We are grateful to F. Guyot for help with the ion milling, Ph. Blanc for the electron microscopy study, the sample coating, and fruitful discussions. One of us (M.E.) acknowledges financial support from the French Ministere de la Rechereche et de la Technologie.

*Permanent address: High Pressure Physics Institute, Academy of Sciences of Russia, 142092 Troitsk, Russia.

[1] L. Vel, G. Demazeau, and J. Etourneau, Mater. Sci. Eng. B **10**, 149 (1991).

[2] *Synthesis and Properties of Boron Nitride,* edited by J. J. Pouch and S. A. Alteroviz (Trans Tech, Aedermannsdorf, Switzerland, 1990); Mater. Sci. Forum **54&55**, 1 (1990).

[3] Y. N. Xu and W. Y. Ching, Phys. Rev. B **44**, 7787 (1991).

[4] N. Miyata, K. Moriki, O. Mishima, M. Fujisawa, and T. Hattori, Phys. Rev. B **40**, 12 028 (1989).

[5] R. M. Chrenko, Solid State Commun. **14**, 511 (1974).

[6] P. J. Gielisse, S. S. Mitra, J. N. Plendl, R. D. Griffis, L. C. Mansur, R. Marshall, and E. A. Pascoe, Phys. Rev. **155**, 1039 (1967).

[7] A. I. Lukomskii, V. B. Shipilo, E. M. Shishonok, and N. G. Anichenko, Phys. Status Solidi A **102**, K137 (1987).

[8]A. D. Alvarenga, M. Grimsditch, and A. Polian, J. Appl. Phys. **72**, 1955 (1992).
[9]T. Sahu, S. K. Nayak, and R. N. Acharya, Physica B **173**, 257 (1991).
[10]M. Grimsditch, E. S. Zouboulis, and A. Polian, J. Appl. Phys. **76**, 832 (1994).
[11]I. S. Gladkaja, G. A. Dubitzkii, and V. N. Slesarev, Acta Crystallogr. Sect. A **34**, S214 (1978).
[12]D. W. Berreman, Phys. Rev. **130**, 2193 (1963).
[13]S. Iwasa, I. Balslev, and E. Burstein, in *Proceedings of the 7th International Conference on the Physics of Semiconductors, Paris, 1964,* edited by M. Hulin (Dunod, Paris, 1964), p. 1077.
[14]O. S. Heavens, Rep. Prog. Phys. **23**, 1 (1960).
[15]S. H. Wemple and M. DiDomenico, Phys. Rev. B **3**, 1338 (1971).
[16]G. Martinez, in *Handbook of Semiconductors,* edited by M. Balkanski (North-Holland, Amsterdam, 1980), Vol. 2, p. 181.